Infrared Spectra of Oxygen-Rich Yttrium and Lanthanum Dioxygen/Ozonide Complexes in Solid Argon

Yu Gong, Chuanfan Ding, and Mingfei Zhou*

Department of Chemistry, Shanghai Key Laboratory of Molecular Catalysts and Innovative Materials, Advanced Materials Laboratory, Fudan University, Shanghai 200433, China

Received: June 10, 2009

The reactions of yttrium and lanthanum atoms with O_2 have been reinvestigated using matrix isolation infrared spectroscopy and theoretical calculations. The ground-state yttrium and lanthanum atoms react with O_2 to produce the inserted yttrium and lanthanum dioxide molecules as the initial products. The yttrium dioxide molecule interacts spontaneously with additional O_2 molecules to form the oxygen-rich OY(η^2-O_3) complex and possibly the (η^2-O_2)Y(η^2-O_3)$_2$ complexes upon sample annealing, which can be regarded as the side-on bonded yttrium monoxide ozonide complex and the superoxo yttrium bisozonide complex, respectively. Visible irradiation induces the isomerization of the OY(η^2-O_3) complex to the superoxo yttrium peroxide Y(η^2-O_2)$_2$ isomer, in which both the superoxo and peroxo ligands are side-on bonded to the yttrium center. The lanthanum dioxide molecule reacts with additional O_2 molecules to form the lanthanum dioxide−dioxygen complex with planar C_{2v} symmetry, which rearranges to the lanthanum monoxide ozonide complex, OLa(η^2-O_3), under near-infrared excitation.

Introduction

Transition-metal oxides and dioxygen complexes are important intermediates, products, or both involved in a wide range of catalytic and biological processes. The geometric and electronic structures of simple transition-metal oxides and dioxygen complexes have been the subject of considerable experimental as well as theoretical investigations. Group III transition metals possess the simplest electronic structure with only three valence electrons. Therefore, simple group III transition-metal oxides and dioxygen complexes may serve as the starting points for understanding the metal−oxygen bonding in other more complicated transition-metal systems.

Mononuclear transition-metal oxides and dioxygen complexes involving scandium, yttrium, and lanthanum have been studied both experimentally[1−10] and theoretically.[11−26] However, most studies are focused on simple monoxide and dioxide species, and the higher oxygen-rich molecules have attracted less attention. Previous matrix isolation infrared spectroscopic studies indicate that two structures of TMO_3 (TM = Sc, Y, and La), a (O_2)TMO metal monoxide−dioxygen complex, and a TM(O_3) ozonide complex were observed in solid matrixes.[1,6] The (O_2)ScO and (O_2)LaO complexes were proposed to be the photodetachment products of the ScO_3^- and LaO_3^- anions in the photoelectron spectroscopic studies, whereas the ozonide complex was identified in the photoelectron spectroscopic study of YO_3.[2,5] The TMO_4 species were also reported from reactions of laser-ablated metal atoms with O_2 in solid argon matrix. The observed ScO_4 and YO_4 species were attributed to the bisdioxygen complexes, whereas the observed LaO_4 molecule was assigned to a lanthanum dioxide−dioxygen complex.[1,6] The YO_5 and LaO_5 complexes were reported in the gas-phase photoelectron spectroscopic studies. The photoelectron spectra were quite broad and featureless. The floppy (O_2)$_2$YO complex was tentatively assigned as the major isomer from the spectrum of YO_5^- anion, whose geometry may be significantly changed upon detachment of the electron.[2] No structural information can be derived from the PES spectrum of LaO_5.[5]

We have recently reinvestigated the reactions of scandium atoms with O_2 in solid argon. A series of oxygen-rich scandium oxide/dioxygen complexes were formed and characterized.[27] It was found that ground-state scandium atoms react spontaneously with two dioxygen molecules to form the OSc(η^2-O_3) complex, which isomerizes to the more stable Sc(η^2-O_2)$_2$ isomer under visible light excitation. Moreover, the condensing matrix allows for the formation of further oxygen-rich Sc(η^2-O_2)$_3$ and (η^2-O_2)Sc(η^2-O_3)$_2$ clusters, which reveal a rich structure and bonding properties. In this article, we provide a matrix isolation infrared spectroscopic and theoretical study on the reactions of yttrium and lanthanum atoms with O_2. Oxygen-rich YO_4, YO_8, and LaO_4 complexes were formed and characterized, which exhibit a series of new structural motifs.

Experimental and Computational Methods

The experimental setup for pulsed laser-evaporation and matrix isolation infrared spectroscopic investigation has previously been described in detail.[28] Briefly, the 1064 nm fundamental of a Nd/YAG laser (Continuum, Minilite II, 10 Hz repetition rate, and 6 ns pulse width) was focused onto a rotating yttrium or lanthanum target through a hole in a CsI window cooled normally to 6 K by means of a closed-cycle helium refrigerator (ARS, 202N). The laser-evaporated metal atoms were codeposited with dioxygen/argon mixtures onto the CsI window. In general, matrix samples were deposited for 1 h at a rate of approximately 4 mmol/h. The O_2/Ar mixtures were prepared in a stainless steel vacuum line using standard manometric technique. Isotopic $^{18}O_2$ (ISOTEC, 99%) was used without further purification. The infrared absorption spectra of the resulting samples were recorded on a Bruker IFS 66 V spectrometer at 0.5 cm^{-1} resolution between 4000 and 400 cm^{-1} using a liquid-nitrogen-cooled HgCdTe (MCT) detector. Samples were annealed to different temperatures and cooled back to 6

* Corresponding author. E-mail: mfzhou@fudan.edu.cn.

10.1021/jp905428s CCC: $40.75
Published on Web 07/06/2009

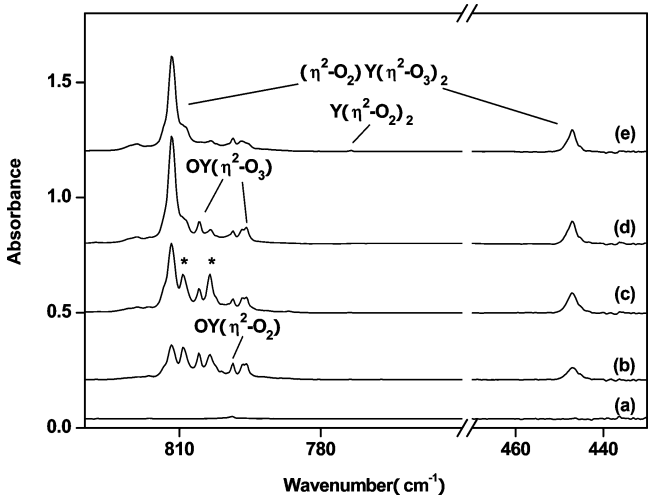

Figure 1. Infrared spectra in the 830−750 and 470−430 cm^{-1} regions from codeposition of laser-evaporated yttrium atoms with 0.5% O_2 in argon. (a) 1 h of sample deposition at 6 K, (b) after 25 K annealing, (c) after 35 K annealing, (d) after 40 K annealing, and (e) after 10 min of $\lambda > 500$ nm irradiation. The asterisks denote the site absorptions of the $(\eta^2\text{-}O_2)Y(\eta^2\text{-}O_3)_2$ complex.

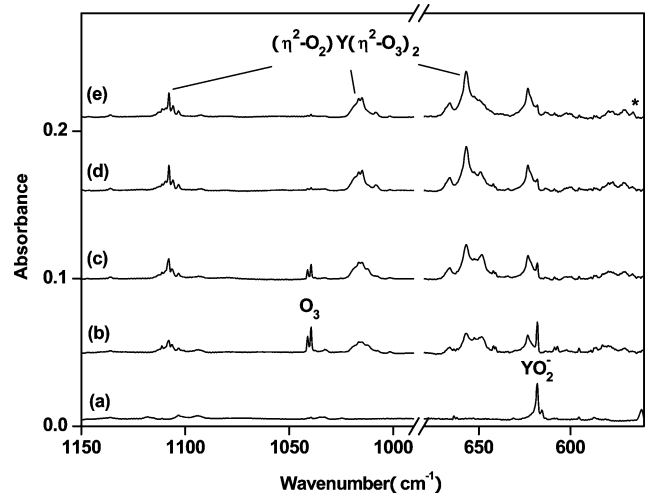

Figure 2. Infrared spectra in the 1150−990 and 680−560 cm^{-1} regions from codeposition of laser-evaporated yttrium atoms with 0.5% O_2 in argon. (a) 1 h of sample deposition at 6 K, (b) after 25 K annealing, (c) after 35 K annealing, (d) after 40 K annealing, and (e) after 10 min of $\lambda > 500$ nm irradiation. The asterisk denotes the absorption of the $Y(\eta^2\text{-}O_2)_2$ complex.

K for spectral acquisition, and selected samples were subjected to broadband irradiation using a tungsten lamp with glass filters. Typically the infrared spectra were recorded with 150−200 scans.

Quantum chemical calculations were performed to predict the geometric structures and vibrational frequencies of the potential products to support the experimental assignments. The three-parameter hybrid functional according to Becke with additional correlation corrections due to Lee, Yang, and Parr (B3LYP) and the nonlocal exchange functional according to Becke with additional correlation corrections due to Perdew (BP86) were utilized.[29,30] The 6-311+G(d) basis set was used for the O atoms, and the scalar-relativistic SDD pseudopotential and basis set was used for the Y and La atoms.[31,32] The geometries were fully optimized, the harmonic vibrational frequencies were calculated, and zero-point vibrational energies (ZPVE) were derived. All calculations were performed using the Gaussian 03 program.[33]

Results and Discussions

A series of experiments were performed using different O_2 concentrations. The O_4^- anion[34] and O_3 absorptions were observed in the experiments using high O_2 concentrations with both the yttrium and lanthanum targets. The O_4^- anion appeared after sample deposition but decreased upon subsequent annealing, during which the O_3 absorption increased. The O_3 molecule is formed via the $O_2 + O$ reaction in solid argon. The oxygen atom is formed from O_2 dissociation during the condensation process.

Y + O_2. The infrared spectra in selected regions from codeposition of laser-evaporated yttrium atoms and 0.5% O_2 are shown in Figures 1 and 2. After 1 h of sample deposition at 6 K, yttrium-based product absorptions at 843.2, 708.2, 702.2, and 618.1 cm^{-1} were observed. The 843.2 and 708.2 cm^{-1} absorptions were attributed to the diatomic YO and inserted bent YO_2 molecules.[6] The 702.2 and 618.1 cm^{-1} absorptions were previously assigned to the symmetric (ν_1) and antisymmetric (ν_3) stretching modes of the bent YO_2^- anion.[6] A 872.0 cm^{-1} absorption produced on UV irradiation was previously assigned to the YO^+ cation, but recent study in our laboratory suggested that the YO^+ cation is chemically coordinated by six argon atoms in solid argon, and the 872.0 cm^{-1} absorption should be regarded as the $[YO(Ar)_6]^+$ complex instead of the bare diatomic cation.[35] The absorptions of ions and YO decreased upon sample annealing, during which a series of new absorptions were produced. The absorptions at 805.6 and 795.7 cm^{-1} appeared on 25 K annealing and remained almost unchanged on subsequent sample annealing to higher temperatures (Figure 1, traces b−d). Broad band irradiation using the tungsten lamp with a $\lambda > 500$ nm long wavelength pass filter destroyed the 805.6 and 795.7 cm^{-1} absorptions with the formation of three new absorptions at 1104.5, 773.6, and 565.8 cm^{-1}. The 1107.9, 1014.9, 811.6, 656.9, and 447.0 cm^{-1} absorptions also appeared on 25 K annealing, increased remarkably upon higher temperature annealing, and dominate the spectra after sample annealing to 40 K (Figures 1 and 2). However, these absorptions are barely observed in the experiments with very low O_2 concentrations (0.05%). The newly observed product absorptions in the Y + O_2 reaction are listed in Table 1.

La + O_2. The infrared spectra in selected regions from codeposition of laser-evaporated lanthanum atoms with 0.5% O_2 in argon are shown in Figures 3 and 4. Weak metal-dependent absorptions due to LaO (796.7 cm^{-1}), LaO^+ (838.0 cm^{-1}), $OLaO^-$ (652.2 and 559.0 cm^{-1}), and $(O_2)LaO$ (757.8 and 1123.5 cm^{-1}) were observed in the spectrum after sample deposition.[6] Subsequent sample annealing allowed the spontaneous formation of the lanthanum dioxide molecule and the $(\eta^2\text{-}O_2)LaO_2$ complex absorptions, which have previously been reported.[6] As shown in Figure 3, three absorptions at 2208.6, 1403.9, and 1305.9 cm^{-1} are found to track with the $(O_2)LaO_2$ absorptions throughout the experiment. In addition, two new absorptions at 792.0 and 763.9 cm^{-1} were observed, which increased slightly upon annealing to higher temperatures. The intensities of these two absorptions are strongly enhanced at the expense of the $(O_2)LaO_2$ complex upon being exposed to near infrared irradiation with photons in the range of $\lambda > 850$ nm (Figure 4). The newly observed product absorptions in the La + O_2 reaction are also listed in Table 1.

The experiments were repeated under similar experimental conditions using isotopic substituted $^{18}O_2$, $^{16}O_2 + {}^{18}O_2$ (1:1),

TABLE 1: Infrared Absorptions (inverse centimeters) of the Products in Solid Argon

	$^{16}O_2$	$^{18}O_2$	$^{16}O_2+^{16}O_2$	$^{16}O_2+^{16}O^{18}O+^{16}O_2$
OY(η^2-O_3)	805.6	766.8	805.6, 766.8	805.6, 767.0
	795.7	751.6	795.7, 786.4, 761.3, 751.6,	795.7, 786.4, 776.9, 771.2, 761.3, 751.6
Y(η^2-O_2)$_2$	1104.5	1042.3	1104.5, 1073.9, 1042.3	1104.5, 1073.9, 1042.3
	773.6	731.6	773.6, 753.3, 731.6	773.6, 753.3, 731.6
	565.8	541.0	585.8, 556.3, 541.0	565.8, 556.3, 541.0
(η^2-O_2)Y(η^2-O_3)$_2$	1107.9	1045.2	1107.9, 1045.2	1107.9, 1077.1, 1045.2
	1106.2[a]	1043.6	1106.4, 1043.7	1106.4, 1075.6, 1043.9
	1014.9	958.9	1016.5, 1008.6, 1002.4, 976.8, 971.7, 960.5	
	811.6	766.8	811.6, 804.6, 801.6, 795.5, 777.1, 766.8	
	809.2[a]	764.4	809.2, 802.5, 801.1, 792.2, 774.6, 764.4	
	803.5[a]	759.1		
	656.9	621.6		
	447.0	429.3	446.9, 429.8	446.5, 434.4, 429.6
	445.2[a]	428.1	445.2, 428.1	445.2, 433.5, 427.9
(η^2-O_2)LaO_2	2208.6	2085.9	2208.4, 2085.9	2208.6, 2148.2, 2085.9
	2204.6[a]	2081.2	2203.8, 2081.1	2204.0, 2144.7, 2081.1
	1403.9	1330.1	1403.6, 1330.4	1403.4, 1367.4, 1330.7
	1305.9	1233.1		
	1111.1	1048.6	1110.5, 1048.1	1110.6, 1080.3, 1048.2
	1109.3[a]	1046.7	1108.6, 1046.5	1108.9, 1078.4, 1046.7
	602.9	574.5	602.0, 574.5	602.0, 590.1, 574.5
OLa(η^2-O_3)	792.0	748.0	792.0, 782.6, 757.6, 748.0	792.0, 782.6, 773.2, 767.5, 757.6, 748.0
	788.9[a]	745.0	788.9, 779.6, 754.7, 745.1	788.9, 779.6, 770.1, ...,[b] 754.8, 745.1
	763.9	724.6	763.7, 724.6	763.9, 724.7
764.8[a]	725.7	764.8, 725.7	764.5, 725.7	

[a] Site absorptions. [b] Unresolved absorption due to band overlap.

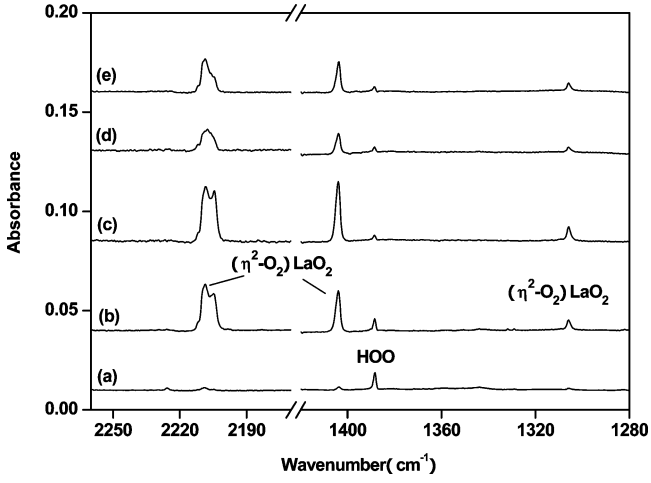

Figure 3. Infrared spectra in the 2260−2170 and 1420−1280 cm^{-1} regions from codeposition of laser-evaporated lanthanum atoms with 0.5% O_2 in argon. (a) 1 h of sample deposition at 6 K, (b) after 25 K annealing, (c) after 40 K annealing, (d) after 10 min of $\lambda > 850$ nm irradiation, and (e) after 35 K annealing.

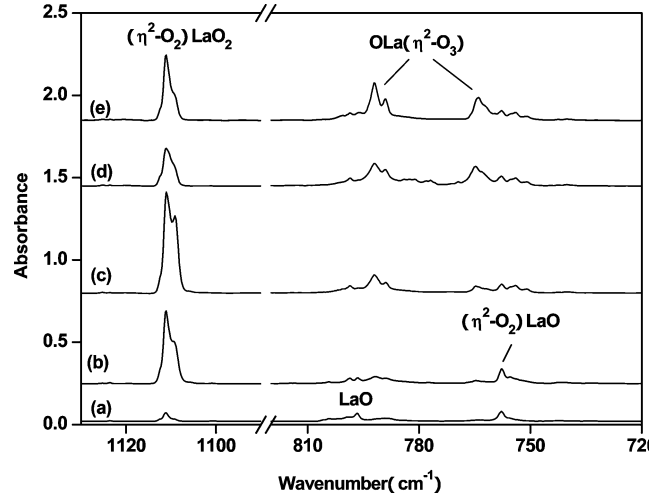

Figure 4. Infrared spectra in the 1130−1090 and 820−720 cm^{-1} regions from codeposition of laser-evaporated lanthanum atoms with 0.5% O_2 in argon. (a) 1 h of sample deposition at 6 K, (b) after 25 K annealing, (c) after 40 K annealing, (d) after 10 min of $\lambda > 850$ nm irradiation, and (e) after 35 K annealing.

and $^{16}O_2$ +$^{16}O^{18}O$ + $^{18}O_2$ (1:2:1) samples to help product identifications. The spectra in selected regions with different isotopic samples are shown in Figures 5−7, respectively. The isotopic counterparts of the observed product absorptions are also summarized in Table 1.

OM(η^2-O_3) (M = Y, La). The 805.6 and 795.7 cm^{-1} absorptions were tentatively assigned to the $(O_2)_x$YO and YO_3 complexes in previous matrix isolation experiments.[6] The present experiments reveal that these two absorptions exhibit identical behaviors throughout all experiments, which indicates that these absorptions should belong to different vibrational modes of the same species. The 805.6 cm^{-1} absorption shifted to 766.8 cm^{-1} with the $^{18}O_2$ sample. The resulting $^{16}O/^{18}O$ isotopic frequency ratio (1.0506) is characteristic of a terminal Y═O stretching vibration. No intermediate absorption was observed in the mixed $^{16}O_2$ + $^{18}O_2$ and $^{16}O_2$ +$^{16}O^{18}O$ + $^{18}O_2$ experiments, implying that only one YO fragment is involved in this mode (Figure 5). In agreement with previous report,[6] the isotopic data for the 795.7 cm^{-1} absorption indicates that this absorption is due to an O−O stretching vibration. This mode splits into a quartet and a sextet in the spectra using the mixed $^{16}O_2$ + $^{18}O_2$ and $^{16}O_2$ + $^{16}O^{18}O$ + $^{18}O_2$ samples, respectively (Figure 5). The band position and mixed isotopic features imply that this absorption is due to the antisymmetric O−O stretching vibration of a side-on bonded O_3 subunit. Accordingly, we assign the 805.6 and 795.7 cm^{-1} absorptions to the OY(η^2-O_3) complex following the example of the OSc(η^2-O_3) complex. Similar absorptions at 763.9 and 792.0 cm^{-1} in the La + O_2 experiments are assigned to the La═O and antisymmetric O−O stretching modes of the OLa(η^2-O_3) complex.

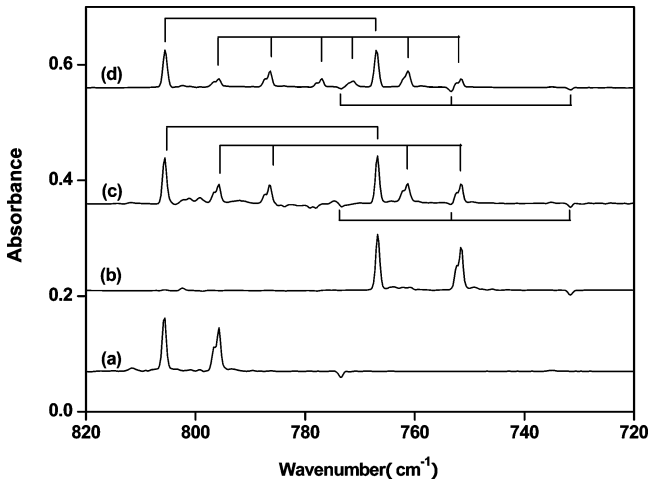

Figure 5. Difference IR spectra in the 820−720 cm^{-1} region from codeposition of laser-evaporated yttrium atoms with different isotopic samples (spectra taken after 10 min $\lambda > 500$ nm irradiation minus spectra taken after 40 K annealing). (a) 0.1% $^{16}O_2$, (b) 0.1% $^{18}O_2$, (c) 0.05% $^{16}O_2$ + 0.05% $^{18}O_2$, and (d) 0.025% $^{16}O_2$ + 0.05% $^{16}O^{18}O$ + 0.025% $^{18}O_2$. Bands upward denote the absorptions of the OY(η^2-O_3) complex, and bands downward denote the absorptions of the Y(η^2-O_2)$_2$ complex.

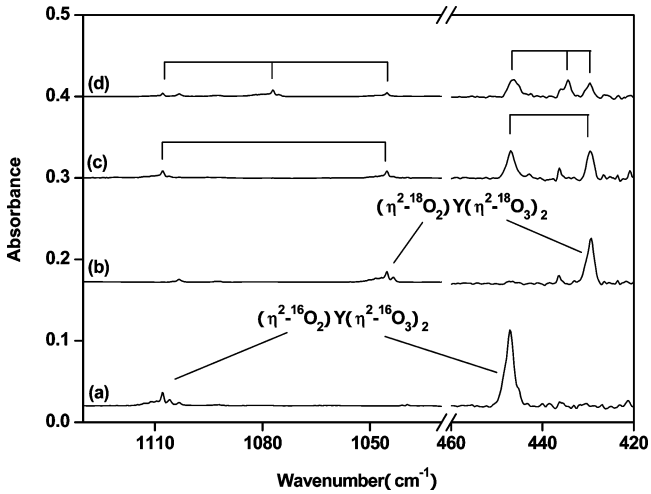

Figure 6. Infrared spectra in the 1130−1030 and 460−420 cm^{-1} regions from codeposition of laser-evaporated yttrium atoms with isotopic-labeled O_2 in excess argon. Spectra were taken after 10 min of $\lambda > 500$ nm irradiation. (a) 0.5% $^{16}O_2$, (b) 0. 5% $^{18}O_2$, (c) 0.25% $^{16}O_2$ + 0.25% $^{18}O_2$, and (d) 0.125% $^{16}O_2$ + 0.25% $^{16}O^{18}O$ + 0.125% $^{18}O_2$.

Our assignment of the OM(η^2-O_3) (M = Y and La) complex is strongly supported by density functional calculations. As shown in Figure 8, both complexes were found to have a $^2A'$ ground state with nonplanar C_s symmetry, in which the terminal MO bond bends out of the MO_3 plane. The terminal Y═O and La═O bond lengths were calculated to be 1.840 and 1.844 Å, respectively, similar to the values predicted for other species with terminal M═O bonds.[36] The experimentally observed M═O and antisymmetric O−O stretching vibrations were calculated to have the largest infrared intensities, with the other modes being much weaker (Table 2). As listed in Table 3, both the calculated frequencies and isotopic frequency ratios are in good agreement with the experimental values.

The OM(η^2-O_3) complexes have been experimentally identified for all three group III metals.[27] The predicted terminal M═O bond lengths are quite similar for yttrium and lanthanum, and both are about 0.17 Å longer than that of scandium, which is

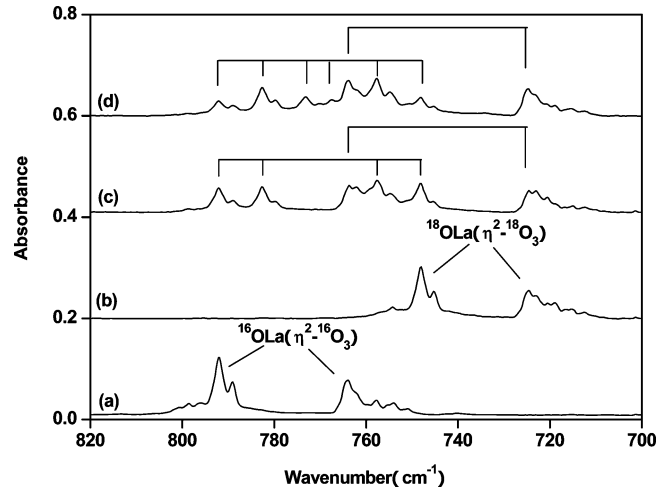

Figure 7. Infrared spectra in the 820−700 cm^{-1} region from codeposition of laser-evaporated lanthanum atoms with isotopic-labeled O_2 in excess argon. Spectra were taken after 10 min of $\lambda > 850$ nm irradiation followed by 35 K annealing. (a) 0.5% $^{16}O_2$, (b) 0. 5% $^{18}O_2$, (c) 0.25% $^{16}O_2$ + 0.25% $^{18}O_2$, and (d) 0.125% $^{16}O_2$ + 0.25% $^{16}O^{18}O$ + 0.125% $^{18}O_2$.

consistent with the trend for the diatomic molecules. The structural parameters of the O_3 unit are quite similar to those of other recently characterized ozonide complexes, suggesting an anionic nature of the O_3 ligand involved.[37] The calculated Mulliken charges on the O_3 subunit for all three OM(η^2-O_3) complexes are around −0.4 e, comparable to the values predicted for some early transition-metal−ozone complexes using density functional calculations.[38] As has been discussed in OSc(η^2-O_3),[27] these OM(η^2-O_3) complexes can be formally described as electron-transferred $MO^+(O_3)^-$ complexes with the unpaired electron occupying the LUMO of molecular ozone. The diatomic metal monoxide molecules have a $^2\Sigma^+$ ground state with the unpaired electron locating on a nonbonding σ orbital that is mainly metal-based orbital in character. Therefore, the MO bond lengths upon coordination of ozone are only about 0.01 Å longer than those of the diatomic metal monoxide molecules.

Y(η^2-O_2)$_2$. Infrared absorptions at 1104.5, 773.6, and 565.8 cm^{-1} increased upon visible irradiation, during which the OY(η^2-O_3) complex absorptions were destroyed. This experimental observation suggests that the absorber of the 1104.5, 773.6, and 565.8 cm^{-1} absorptions is a structural isomer of OY(η^2-O_3). The isotopic substitution studies indicate that both the 1104.5 and 773.6 cm^{-1} absorptions are due to O−O stretching vibrations. Each absorption split into a triplet in the experiment when a mixed $^{16}O_2$ + $^{16}O^{18}O$ + $^{18}O_2$ (1:2:1 molar ratio) sample was used, indicating that both the 1104.5 and 773.6 cm^{-1} absorptions are originated from two different O_2 ligands. Each O_2 ligand is side-on bonded with two equivalent oxygen atoms. The band position and isotopic frequency ratio of the 565.8 cm^{-1} absorption suggest a Y−O_2 vibration. Accordingly, the absorptions at 1104.5, 773.6, and 565.8 cm^{-1} are attributed to a Y(η^2-O_2)$_2$ complex with two inequivalent O_2 ligands.

To validate the experimental assignment, density functional calculations were performed on the Y(η^2-O_2)$_2$ complex. As shown in Figure 8, the complex was predicted to have an $^2A_2$ ground state with nonplanar C_{2v} symmetry. The complex has two inequivalent O_2 ligands with O−O bond lengths of 1.502 and 1.336 Å, which are close to the values of peroxo dianion and superoxo anion, respectively.[39−41] Therefore, the Y(η^2-O_2)$_2$ complex can be described as a superoxo yttrium peroxide

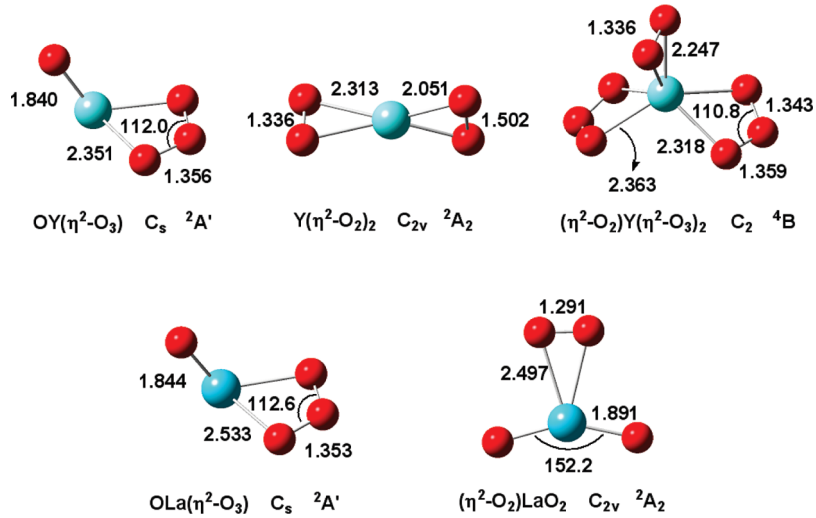

Figure 8. Optimized structures of the products at the DFT/B3LYP level of theory (bond lengths in angstroms and bond angles in degrees). The structural parameters of the (η2-O_2)LaO_2 complex was obtained using the DFT/BP86 method.

TABLE 2: DFT/B3LYP Calculated Total Energies (in hartree, after Zero-Point Energy Corrections), Frequencies (inverse centimeters), and Intensities (kilometers/mole) of the Observed Products

molecule	energy	frequencies (intensity)
$OY(\eta^2\text{-}O_3)$ ($^2A'$, C_s)	−339.188235	1061.1 (2), 854.5 (253), 832.2 (198), 656.9 (25), 308.5 (0), 290.1 (45), 204.6 (11), 111.8 (31), 101.8 (29)
$Y(\eta^2\text{-}O_2)_2$ ($^2A_2$, C_{2v})	−339.210738	1161.4 (34), 816.7 (136), 556.6 (20), 548.9 (66), 420.2 (4), 375.2 (36), 143.5 (0), 42.4 (52), 2.4i(66)[b]
$(\eta^2\text{-}O_2)Y(\eta^2\text{-}O_3)_2$ (^4B, C_2)	−639.975104	1170.0 (13), 1087.4 (4), 1086.6 (15), 867.8 (415), 853.7 (3), 683.9 (17), 673.3 (69), 441.9 (101), 393.7 (2), 336.6 (102), 286.8 (9), 261.7 (4), 246.3 (9), 199.4 (6), 179.7 (2), 79.1 (5), 62.0 (3), 48.9 (12), 47.5 (0), 38.9 (3), 28.3 (0)
$(\eta^2\text{-}O_2)LaO_2$ ($^2A_2$, C_{2v})	−736.551498	1399.1 (733), 578.5 (131), 422.2 (0), 186.9 (0), 169.8 (39), 111.4 (65), 89.4 (1), 71.5 (58), 65.9 (0)
$(\eta^2\text{-}O_2)LaO_2$ ($^2A_2$, C_{2v})	−736.669908[a]	1225.3 (232), 676.5 (155), 591.0 (44), 351.1 (0), 247.7 (17), 191.7 (37), 159.0 (52), 138.8 (0), 86.4 (0)
$OLa(\eta^2\text{-}O_3)$ ($^2A'$, C_s)	−736.567002	1068.2 (1), 851.9 (239), 790.2 (270), 633.3 (37), 241.6(55), 233.7 (0), 166.2 (14), 83.6 (19), 78.3 (25)

[a] Calculated at the DFT/BP86 level of theory. [b] Imaginary frequency produced because of the limitations in the numerical integration procedures used in the DFT computations.

complex with the yttrium center in the +3 oxidation state. The structural characters of the $Y(\eta^2\text{-}O_2)_2$ complex are very similar to the recently reported scandium analog.[27] As listed in Tables 2 and 3, the three experimentally observed absorptions are well reproduced by theoretical calculations.

The YO_4 molecule has been observed as the photodetachment product of the YO_4^- anion in the gas phase, but the spectra were broad and featureless.[2] The low binding energy feature was assigned to the end-on bonded superoxide complex, whereas a peroxide isomer with two side-on bonded O_2 ligands was tentatively assigned as the origination of the feature observed at high binding energy. Similar structure was also proposed in a previous matrix isolation study. A 446.5 cm^{-1} absorption was assigned to the $Y(O_2)_2$ complex with two equivalent O_2 ligands.[6] According to our calculations, these structures are not global minima on the potential energy surface of YO_4; the $Y(\eta^2\text{-}O_2)_2$ complex with one side-on bonded superoxide ligand and one peroxide ligand is the most stable structure with two O_2 ligands bound to the yttrium center. As will be discussed, the previously observed 446.5 cm^{-1} absorption is due to the $(\eta^2\text{-}O_2)Y(\eta^2\text{-}O_3)_2$ complex.

$(\eta^2\text{-}O_2)Y(\eta^2\text{-}O_3)_2$. The 1107.9, 1014.9, 811.6, 656.9, and 447.0 cm^{-1} absorptions are favored at higher O_2 concentrations, suggesting that the absorber should be due to an oxygen-rich complex. The weak absorption at 1107.9 cm^{-1} is assigned to an O−O stretching vibration with two equivalent oxygen atoms on the basis of experimental isotopic shift and splits. The strong infrared absorption at 447.0 cm^{-1} in the low frequency region is the corresponding Y−O_2 stretching vibration. The strong absorption at 811.6 cm^{-1} as well as the weak 1014.9 and 656.9 cm^{-1} absorptions exhibited $^{16}O/^{18}O$ isotopic frequency ratios around 1.058. Note that the band positions are quite close to the antisymmetric and symmetric O−O stretching and bending modes of ozonide complexes, indicating that the absorber also involves O_3 subsunit(s).[37,42] The isotopic splittings in the experiment with equal molar mixtures of $^{16}O_2$ and $^{18}O_2$ are quite complicated and cannot be well-resolved, suggesting the involvement of more than one O_3 subunit. Considering the oxygen-rich nature of these absorptions, a $(\eta^2\text{-}O_2)Y(\eta^2\text{-}O_3)_2$ complex with one side-on bonded O_2 ligand and two side-on bonded O_3 ligands is proposed to be the absorber.

The most stable structure of the $(\eta^2\text{-}O_2)Y(\eta^2\text{-}O_3)_2$ complex predicted at the DFT/B3LYP level of theory is illustrated in Figure 8. The complex was predicted to have C_2 symmetry and a ^4B ground state with its structures about the same as the scandium analog observed in the Sc + O_2 reaction.[27] The O−O bond length of the side-on bonded O_2 ligand was calculated to be 1.336 Å, which falls into the range of a superoxide anion.[39,41] The two O_3 ligands are bound to the yttrium center with two terminal oxygen atoms in a side-on fashion. The $(\eta^2\text{-}O_2)Y(\eta^2\text{-}$

TABLE 3: Comparison Between the Observed and Calculated Vibrational Frequencies (inverse centimeters) and Isotopic Frequency Ratios of the Observed Products

		freq		$^{16}O/^{18}O$	
molecule	mode	calcd	obsd	calcd	obsd
OY(η^2-O_3) ($^2A'$, C_s)	O_3 asym. str. (a″)	854.5	795.7	1.0607	1.0587
	YO str. (a′)	832.2	805.6	1.0510	1.0506
Y(η^2-O_2)$_2$	superoxo O−O str. (a_1)	1161.4	1104.5	1.0607	1.0597
	peroxo O−O str. (a_1)	816.7	773.6	1.0582	1.0574
	Y-peroxo O_2 str. (a_1)	548.9	565.8	1.0445	1.0458
(η^2-O_2)Y (η^2-O_3)$_2$ (^4B, C_2)	O−O str. (a)	1170.0	1107.9	1.0608	1.0600
	O_3 sym. str. (b)	1086.6	1014.9	1.0607	1.0584
	O_3 asym. str. (b)	867.8	811.6	1.0605	1.0584
	O_3 bend. (b)	673.3	656.9	1.0601	1.0568
	Y−O_2 sym. str. (a)	441.9	447.0	1.0400	1.0400
(η^2-O_2)LaO_2	2ν(O−O)		2208.6		1.0588
	combination mode		1403.9		1.0555
	combination mode		1305.9		1.0590
	O−O str. (a_1)	1225.3[a]	1111.1	1.0608	1.0596
	OLaO asym. str. (b_2)	676.5[a]	602.9	1.0487	1.0494
OLa(η^2-O_3) ($^2A'$, C_s)	O_3 asym. str. (a″)	851.9	792.0	1.0608	1.0588
	LaO str. (a′)	790.2	763.9	1.0543	1.0542

[a] Calculated at the DFT/BP86 level of theory. The symmetric OLaO stretching vibration was predicted at 578.5 cm^{-1} using B3LYP with the isotopic ratio of 1.0597 while the antisymmetric stretching vibration was predicted at 422.2 cm^{-1} with very low IR intensity.

$O_3)_2$ complex can be regarded to be a six-fold coordinated superoxo yttrium bisozonide complex. Consistent with this notion, the spin densities are mainly distributed on the O_2 (1.02 e) and two O_3 (0.99 e each) fragments.

(η^2-O_2)LaO_2. The 1111.1 and 602.9 cm^{-1} absorptions were observed in previous matrix isolation experiments and were assigned to the O−O and antisymmetric OLaO stretching vibrations of the (η^2-O_2)LaO_2 complex.[6] Besides these two absorptions, three absorptions at 2208.6, 1403.9, and 1305.9 cm^{-1} were observed to track with the 1111.1 and 602.9 cm^{-1} absorptions in the present experiments. The absorption at 2208.6 cm^{-1} exhibited very similar isotopic frequency ratio with the 1111.1 cm^{-1} absorption and is assigned to the overtone (2ν) of the O−O stretching mode. The anharmonic term was determined to be 13.6 cm^{-1}. The 1403.9 and 1305.9 cm^{-1} absorptions are also due to overtone or combination modes of the (η^2-O_2)LaO_2 complex.

We carried out geometry optimizations on the doublet and quartet spin states of the (η^2-O_2)LaO_2 complex with both planar and nonplanar C_{2v} symmetry at the DFT/B3LYP level of theory. It was found that an $^2A_2$ state with planar symmetry is lowest in energy. However, the calculated vibrational frequencies and intensities do not match the experimental observations. The O−O stretching vibration was predicted at 1399.1 cm^{-1}, about 25% higher than the experimentally value. The nonobserved symmetric OLaO stretching mode was calculated to be much intense than the experimentally observed antisymmetric stretching mode. Obviously, the La−O_2 interaction in the (η^2-O_2)LaO_2 complex is underestimated by the hybrid B3LYP functional. In this circumstance, calculations were repeated using pure DFT method with the BP86 functional. At this level of theory, the planar $^2A_2$ state was also predicted to be the ground state of the (η^2-O_2)LaO_2 complex, and the O−O stretching vibration was calculated at 1225.3 cm^{-1}, more close to the experimental value. In addition, the antisymmetric OLaO stretching vibration was predicted to be stronger than the symmetric one, which agrees with the experimental observations. The O−O stretching vibrational frequency as well as the predicted O−O bond length (1.291 Å) indicate that (η^2-O_2)LaO_2 is a superoxide complex.[39,41]

The LaO_4 molecule has been observed in the gas-phase photoelectron spectroscopic experiment.[5] A planar bisdioxygen complex structure with D_{2h} symmetry was proposed to be the ground state of the LaO_4 molecule. Our density functional calculations revealed that the D_{2h} structure with two equivalent O_2 molecules is not a stable isomer. No absorptions can be assigned to such complexes in our experiments.

SCHEME 1

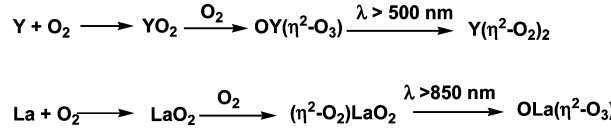

Reaction Mechanisms. Laser-evaporated yttrium and lanthanum atoms react with O_2 spontaneously in forming the inserted dioxide molecules upon sample annealing, as observed in the previous experiments.[6] Annealing the condensing matrix allows the initial products to react with additional reagent O_2 molecules with the formation of further oxygen-rich complexes. The reactions between yttrium and lanthanum metal atoms and dioxygen are summarized in Scheme 1. In the Y + O_2 reaction system, the OY(η^2-O_3) complex absorptions increased on sample annealing, indicating that the primary formed inserted yttrium dioxide molecule reacts spontaneously with another dioxygen to form the OY(η^2-O_3) complex. Both the YO and O_3 species were observed in the experiments with relatively high O_2 concentrations (0.5%), and the formation of OY(η^2-O_3) from the YO + O_3 reaction cannot be ruled out. However, the O_3 absorption is barely observed in the experiments with low O_2 concentrations (<0.1%), whereas the OY(η^2-O_3) absorptions were still produced as the major product absorptions on annealing. The Y(η^2-O_2)$_2$ complex absorptions were produced at the expense of the OY(η^2-O_3) absorptions under $\lambda > 500$ nm light irradiation, which implies that the OY(η^2-O_3) complex isomerizes to the Y(η^2-O_2)$_2$ isomer upon excitation. The infrared spectrum from the mixed $^{16}O_2 + {}^{18}O_2$ (1:1) experiment (Figure 5, trace c) also supports this isomerization mechanism. DFT/B3LYP calculations reveal that this isomerization reaction is thermodynamically favored (14.1 kcal/mol) and is hampered kinetically with the existence of an energy barrier of 19.7 kcal/mol. Therefore, the production of the more stable Y(η^2-O_2)$_2$ complex from OY(η^2-O_3) requires photoexcitation.

In the lanthanum and dioxygen reaction, the lanthanum dioxide−dioxygen complex absorptions dominate the spectrum

when the as-deposited sample was annealed. Our DFT/BP86 calculations revealed that the spontaneous reaction between lanthanum dioxide and O_2 to form the $(\eta^2\text{-}O_2)LaO_2$ complex is exothermic by 9.9 kcal/mol. The $OLa(\eta^2\text{-}O_3)$ absorptions increased when the sample was subjected to near-infrared irradiation at the expense of the $(\eta^2\text{-}O_2)LaO_2$ complex, suggesting that the $(\eta^2\text{-}O_2)LaO_2$ complex is the precursor for the formation of the $OLa(\eta^2\text{-}O_3)$ isomer. In the Sc + O_2 and Y + O_2 reaction systems, no $(\eta^2\text{-}O_2)ScO_2$ and $(\eta^2\text{-}O_2)YO_2$ complexes were experimentally identified.[27] The $(\eta^2\text{-}O_2)ScO_2$ and $(\eta^2\text{-}O_2)YO_2$ complexes are assumed to be potential intermediates involved in the formation of the $OSc(\eta^2\text{-}O_3)$ and $OY(\eta^2\text{-}O_3)$ complexes. The spontaneous formation of the $OSc(\eta^2\text{-}O_3)$ and $OY(\eta^2\text{-}O_3)$ complexes on annealing suggests that the $(\eta^2\text{-}O_2)ScO_2$ and $(\eta^2\text{-}O_2)YO_2$ complexes may not be able to be stabilized in solid argon matrix.

At high O_2 concentration experiments, the $OY(\eta^2\text{-}O_3)$ complex can further react with additional dioxygen molecules to produce the $(\eta^2\text{-}O_2)Y(\eta^2\text{-}O_3)_2$ complex on sample annealing, which was estimated to be exothermic by 33.6 kcal/mol. Besides the $(\eta^2\text{-}O_2)Sc(\eta^2\text{-}O_3)_2$ complex, a $Sc(\eta^2\text{-}O_2)_3$ complex which was characterized to have a $^4A_1''$ ground state with D_{3h} symmetry was also observed to be an oxygen-rich product in the Sc + O_2 reaction.[27] The $Y(\eta^2\text{-}O_2)_3$ and $La(\eta^2\text{-}O_2)_3$ complexes are also expected to be formed in the present Y + O_2 and La + O_2 experiments. However, the most intense IR absorptions of the $La(\eta^2\text{-}O_2)_3$ complex lie out of the spectral range of the spectrometer (>400 cm^{-1}), whereas the $Y(\eta^2\text{-}O_2)_3$ absorptions may also be overlapped by the strong $(\eta^2\text{-}O_2)Y(\eta^2\text{-}O_3)_2$ absorptions.

Conclusions

The reactions of yttrium and lanthanum atoms with dioxygen have been reinvestigated using matrix isolation infrared spectroscopy and density functional theory calculations. Oxygen-rich YO_4, YO_8, and LaO_4 complexes were prepared and characterized. The yttrium and lanthanum atoms react with O_2 spontaneously in forming the inserted dioxide molecules upon sample annealing. Sample annealing allows the initial products to react with additional reagent O_2 molecules to form oxygen-rich complexes. The yttrium dioxide molecule reacts spontaneously with O_2 to form the yttrium monoxide ozonide complex, $OY(\eta^2\text{-}O_3)$. In addition, the superoxo yttrium bisozonide complex, $(\eta^2\text{-}O_2)Y(\eta^2\text{-}O_3)_2$, is also tentatively assigned. The $OY(\eta^2\text{-}O_3)$ complex isomerizes to the superoxo yttrium peroxide complex, $Y(\eta^2\text{-}O_2)_2$ upon visible irradiation. The lanthanum dioxide molecule interacts with additional O_2 to form the lanthanum dioxide−dioxygen complex, which is the precursor for the formation of the $OLa(\eta^2\text{-}O_3)$ isomer under near-infrared irradiation.

Acknowledgment. This work is supported by NKBRSF (grant nos. 2004CB719501 and 2007CB815203) and the National Natural Science Foundation of China (grant no. 20773030).

References and Notes

(1) Chertihin, G. V.; Andrews, L.; Rosi, M.; Bauschlicher, C. W., Jr. *J. Phys. Chem. A* **1997**, *101*, 9085. (a) Bauschlicher, C. W.Jr.; Zhou, M. F.; Andrews, L.; Johnson, J. R. T.; Panas, I.; Snis, A.; Roos, B. O. *J. Phys. Chem. A* **1999**, *103*, 5463.

(2) Wu, H. B.; Wang, L. S. *J. Phys. Chem. A* **1998**, *102*, 9129.

(3) Knight, L. B.; Kaup, J. G.; Petzoldt, B.; Ayyad, R.; Ghanty, T. K.; Davidson, E. R. *J. Chem. Phys.* **1999**, *110*, 5658.

(4) (a) Weltner, W., Jr.; McLeod, D., Jr.; Kasai, P. H. *J. Chem. Phys.* **1967**, *46*, 3172. (b) Kasai, P. H.; Weltner, W., Jr. *J. Chem. Phys.* **1965**, *43*, 2553.

(5) Klingeler, R.; Lüttgens, G.; Pontius, N.; Rochow, R.; Bechthold, P. S.; Neeb, M.; Eberhardt, W. *Eur. Phys. J. D* **1999**, *9*, 263.

(6) Andrews, L.; Zhou, M. F.; Chertihin, G. V.; Bauschlicher, C. W., Jr. *J. Phys. Chem. A* **1999**, *103*, 6525.

(7) (a) Hoeft, J.; Törring, T. *Chem. Phys. Lett.* **1993**, *215*, 367. (b) Törring, T.; Zimmermann, K.; Hoeft, J. *Chem. Phys. Lett.* **1988**, *151*, 520.

(8) Howard, J. A.; Histed, M.; Mile, B.; Hampson, C. A.; Morris, H. *J. Chem. Soc., Faraday Trans.* **1991**, *87*, 3189.

(9) Suenram, R. D.; Lovas, F. J.; Fraser, G. T.; Matsumura, K. *J. Chem. Phys.* **1990**, *92*, 4724.

(10) Merer, A. J. *Annu. Rev. Phys. Chem.* **1989**, *40*, 407.

(11) Harrison, J. F. *Chem. Rev.* **2000**, *100*, 679.

(12) (a) Gutsev, G. L.; Andrews, L.; Bauschlicher, C. W., Jr. *Theor. Chem. Acc.* **2003**, *109*, 298. (b) Gutsev, G. L.; Rao, B. K.; Jena, P. *J. Phys. Chem. A* **2000**, *104*, 11961. (c) Langhoff, S. R.; Bauschlicher, C. W., Jr. *J. Chem. Phys.* **1988**, *89*, 2160.

(13) Uzunova, E. L.; Mikosch, H.; Nikolov, G. St. *J. Chem. Phys.* **2008**, *128*, 094307.

(14) (a) Rosi, M.; Bauschlicher, C. W.; Chertihin, G. V.; Andrews, L. *Theor. Chem. Acc.* **1998**, *99*, 106.

(15) Kim, S. J.; Crawford, T. D. *J. Phys. Chem. A* **2004**, *108*, 3097.

(16) Gonzales, J. M.; King, R. A.; Schaefer, H. F., III *J. Chem. Phys.* **2000**, *113*, 567.

(17) Johnson, J. R. T.; Panas, I. *Chem. Phys.* **1999**, *248*, 161.

(18) (a) Lee, E. P. F.; Mok, D. K. W.; Chau, F. T.; Dyke, J. M. *J. Comput. Chem.* **2008**, *30*, 337. (b) Lee, E. P. F.; Dyke, J. M.; Mok, D. K. W.; Chau, F.-T. *J. Phys. Chem. A* **2008**, *112*, 4511. (c) Todorova, T. K.; Infante, I.; Gagliardi, L.; Dyke, J. M. *J. Phys. Chem. A* **2008**, *112*, 7825.

(19) (a) Siegbahn, P. E. M. *Chem. Phys. Lett.* **1993**, *201*, 15. (b) Siegbahn, P. E. M. *J. Phys. Chem.* **1993**, *97*, 9096.

(20) Kharat, B.; Deshmukh, S. B.; Chaudhari, A. *Int. J. Quantum Chem.* **2009**, *109*, 1103.

(21) (a) Song, P.; Guan, W.; Yao, C.; Su, Z. M.; Wu, Z. J.; Feng, J. D.; Yan, L. K. *Theor. Chem. Acc.* **2007**, *117*, 407. (b) Wu, Z. J.; Guan, W.; Meng, J.; Su, Z. M. *J. Cluster Sci.* **2007**, *18*, 444.

(22) (a) Cao, X.; Dolg, M. *THEOCHEM* **2002**, *581*, 139. (b) Cao, X.; Dolg, M. *J. Chem. Phys.* **2001**, *115*, 7348. (c) Küchle, W.; Dolg, M.; Stoll, H. *J. Phys. Chem. A* **1997**, *101*, 7128. (d) Dolg, M.; Stoll, H. *Theor. Chim. Acta* **1989**, *75*, 369.

(23) (a) Wang, S. G.; Schwarz, W. H. E. *J. Phys. Chem.* **1995**, *99*, 11687. (b) Wang, S. G.; Pan, D. K.; Schwarz, W. H. E. *J. Chem. Phys.* **1995**, *102*, 9296.

(24) Kotzian, M.; Rösch, N.; Zerner, M. C. *Theor. Chim. Acta* **1992**, *81*, 201.

(25) Schamps, J.; Bencheikh, M.; Barthelat, J.-C.; Field, R. W. *J. Chem. Phys.* **1995**, *103*, 8004.

(26) Marquez, A.; Capitan, M. J.; Odriozola, J. A.; Sanz, J. F. *Int. J. Quantum Chem.* **1994**, *52*, 1329.

(27) Gong, Y.; Ding, C. F.; Zhou, M. F. *J. Phys. Chem. A* **2007**, *111*, 11572.

(28) Wang, G. J.; Zhou, M. F. *Int. Rev. Phys. Chem.* **2008**, *27*, 1.

(29) (a) Becke, A. D. *J. Chem. Phys.* **1993**, *98*, 5648. (b) Lee, C.; Yang, W.; Parr, R. G. *Phys. Rev. B* **1988**, *37*, 785.

(30) (a) Becke, A. D. *Phys. Rev. A* **1988**, *38*, 3098. (b) Perdew, J. P. *Phys. Rev. B* **1986**, *33*, 8822.

(31) (a) McLean, A. D.; Chandler, G. S. *J. Chem. Phys.* **1980**, *72*, 5639. (b) Krishnan, R.; Binkley, J. S.; Seeger, R.; Pople, J. A. *J. Chem. Phys.* **1980**, *72*, 650.

(32) (a) Dolg, M.; Stoll, H.; Preuss, H. *J. Chem. Phys.* **1989**, *90*, 1730. (b) Andrae, D.; Haussermann, U.; Dolg, M.; Stoll, H.; Preuss, H. *Theor. Chim. Acta.* **1990**, *77*, 123.

(33) Frisch, M. J.; Trucks, G. W.; Schlegel, H. B.; Scuseria, G. E.; Robb, M. A.; Cheeseman, J. R.; Montgomery, J. A., Jr.; Vreven, T.; Kudin, K. N.; Burant, J. C.; Millam, J. M.; Iyengar, S. S.; Tomasi, J.; Barone, V.; Mennucci, B.; Cossi, M.; Scalmani, G.; Rega, N.; Petersson, G. A.; Nakatsuji, H.; Hada, M.; Ehara, M.; Toyota, K.; Fukuda, R.; Hasegawa, J.; Ishida, M.; Nakajima, T.; Honda, Y.; Kitao, O.; Nakai, H.; Klene, M.; Li, X.; Knox, J. E.; Hratchian, H. P.; Cross, J. B.; Adamo, C.; Jaramillo, J.; Gomperts, R.; Stratmann, R. E.; Yazyev, O.; Austin, A. J.; Cammi, R.; Pomelli, C.; Ochterski, J. W.; Ayala, P. Y.; Morokuma, K.; Voth, G. A.; Salvador, P.; Dannenberg, J. J.; Zakrzewski, V. G.; Dapprich, S.; Daniels, A. D.; Strain, M. C.; Farkas, O.; Malick, D. K.; Rabuck, A. D.; Raghavachari, K.; Foresman, J. B.; Ortiz, J. V.; Cui, Q.; Baboul, A. G.; Clifford, S.; Cioslowski, J.; Stefanov, B. B.; Liu, G.; Liashenko, A.; Piskorz, P.; Komaromi, I.; Martin, R. L.; Fox, D. J.; Keith, T.; Al-Laham, M. A.; Peng, C. Y.; Nanayakkara, A.; Challacombe, M.; Gill, P. M. W.; Johnson, B.; Chen, W.; Wong, M. W.; Gonzalez, C.; Pople, J. A. *Gaussian 03*, revision B.05; Gaussian, Inc.: Pittsburgh, PA, 2003.

(34) Chertihin, G. V.; Andrews, L. *J. Chem. Phys.* **1998**, *108*, 6404.

(35) Zhao, Y. Y.; Gong, Y.; Chen, M. H.; Ding, C. F.; Zhou, M. F. *J. Phys. Chem. A* **2005**, *109*, 11765.

(36) (a) Zhang, L. N.; Shao, L. M.; Zhou, M. F. *Chem. Phys.* **2001**, *272*, 27. (b) Wang, X. F.; Andrews, L. *J. Phys. Chem. A* **2006**, *110*, 4157. (c) Jiang, L.; Xu, Q. *J. Phys. Chem. A* **2008**, *112*, 6289.

(37) (a) Gong, Y.; Zhou, M. F.; Tian, S. X.; Yang, J. L. *J. Phys. Chem. A* **2007**, *111*, 6127. (b) Gong, Y.; Zhou, M. F. *J. Phys. Chem. A* **2007**, *111*, 8973.

(38) (a) Flemmig, B.; Wolczanski, P. T.; Hoffmann, R. *J. Am. Chem. Soc.* **2005**, *127*, 1278. (b) Venter, G. A.; Raubenheimer, H. G.; Dillen, J. *J. Phys. Chem. A* **2007**, *111*, 8193.

(39) Cramer, C. J.; Tolman, W. B.; Theopold, K. H.; Rheingold, A. L. *Proc. Natl. Acad. Sci. U.S.A.* **2003**, *100*, 3635.

(40) (a) Gong, Y.; Zhou, M. F.; Andrews, L. *J. Phys. Chem. A* **2007**, *111*, 12001. (b) Gong, Y.; Zhou, M. F. *J. Phys. Chem. A* **2008**, *112*, 9758. (c) Gong, Y.; Wang, G. J.; Zhou, M. F. *J. Phys. Chem. A* **2008**, *112*, 4936. (d) Gong, Y.; Zhou, M. F. *Chin. J. Chem. Phys.* **2009**, *22*, 113.

(41) (a) Gong, Y.; Wang, G. J.; Zhou, M. F. *J. Phys. Chem. A* **2009**, *113*, 5355. (b) Zhao, Y. Y.; Su, J.; Gong, Y.; Li, J.; Zhou, M. F. *J. Phys. Chem. A* **2008**, *112*, 8606. (c) Zhao, Y. Y.; Zheng, X. M.; Zhou, M. F. *Chem. Phys.* **2008**, *351*, 13. (d) Yang, R.; Gong, Y.; Zhou, H.; Zhou, M. F. *J. Phys. Chem. A* **2007**, *111*, 64. (e) Yang, R.; Gong, Y.; Zhou, M. F. *Chem. Phys.* **2007**, *340*, 134. (f) Zhao, Y. Y.; Gong, Y.; Chen, M. H.; Zhou, M. F. *J. Phys. Chem. A* **2006**, *110*, 1845.

(42) (a) Andrews, L. *J. Am. Chem. Soc.* **1973**, *95*, 4487. (b) Andrews, L.; Spiker, R. C., Jr. *J. Chem. Phys.* **1973**, *59*, 1863. (c) Spiker, R. C., Jr.; Andrews, L. *J. Chem. Phys.* **1973**, *59*, 1851.

JP905428S